"Chemical Photography" of Drug Release

Sergei G. Kazarian* and K. L. Andrew Chan

Department of Chemical Engineering and Chemical Technology, Imperial College London, South Kensington Campus, London SW7 2AZ, United Kingdom

Received August 15, 2003; Revised Manuscript Received October 28, 2003

ABSTRACT: The enhanced chemical visualization of FTIR spectroscopic imaging combined with the macro-ATR−IR approach has allowed us to study polymer/drug formulations in contact with aqueous solution as a function of time. This imaging method enabled the analysis of both the drug and polymer distribution via their corresponding IR bands. The evolution of these images as a function of time was studied to reveal the mechanism of drug release. This method allowed us, for the first time, to spectroscopially image the crystallization of ibuprofen molecularly dispersed in poly(ethylene glycol) (PEG) during the dissolution process in water. The imaging of dissolution of inclusion complexes of the drug in cyclodextrin has shown that this can prevent drug crystallization and enhances dissolution. This FTIR imaging approach has considerable potential for revealing the underlying principles of controlled drug release processes from many pharmaceutical formulations.

Introduction

Drug release is important phenomenon with direct health implications. Drug release from formulations with polymers for oral drug delivery is usually studied by analysis of the total concentration of the drug in solution as a function of time. However, such an approach does not really address the important issue as to whether drug release proceeds via drug diffusion or polymer degradation and cannot delineate how the molecular state of the drug affects the rate of drug release. There is an urgent need to apply advanced experimental techniques capable of obtaining spatially resolved chemical information to probe the dissolution phenomenon and drug release at a molecular level. The process of dissolution and drug release from solid dispersions of drugs in polymers includes diffusion of water into the polymer/drug formulation: polymer swelling, polymer dissolution, diffusion of drug, drug dissolution. These phenomena largely control the drug release process, but the overall process may be very complex and many factors affect the drug release mechanism. Comprehensive reviews with extended bibliography on advanced drug delivery have recently been published,[1−3] where the implications of understanding the drug release mechanism for the prediction, control of the release rate, and manufacturing of the solid dispersion have been discussed,[4] pointing at an urgent need to apply new experimental methods to probe the dissolution phenomenon and drug release at a molecular level. It turns out that the recently emerged FTIR spectroscopic imaging[5−12] can be the method of choice to investigate formulations in contact with aqueous environments and to reveal the underlying principles of this process. Unlike many of the other methods, FTIR spectroscopic imaging provides detailed information concerning the chemical composition due to the inherent ability of IR spectra to provide specific information on the molecular structure of materials. FTIR imaging utilizes the advantage of the focal plane array infrared detector to measure thousands of IR spectra from different locations in the sample and to collect simultaneously spatially resolved chemical information. This is the basis of chemically specific "photography" offered by this method. It should be noted that many methods have been used thus far to gain insight into the mechanism of water uptake, polymer swelling and dissolution, and drug release. Until recently, NMR imaging was the only technique capable of obtaining both chemical and spatial information on dynamic polymer/solvent systems in a noninvasive and nondestructive way.[13−16] However, chemical specificity, spatial resolution, and acquisition times of FTIR imaging are superior to those in NMR imaging. The image acquisition time in FTIR imaging can be significantly less than a minute. Conventional FTIR microscopy via mapping requires long measurement times (usually several hours depending on the measured area)[17] and thus is not suitable for studying dynamic processes. Recently, we have demonstrated that enhanced spatial resolution can be achieved with the ATR (attenuated total reflectance)−IR microscopy using an immersed objective made of a material with high refractive index.[18,19] One of the most exciting opportunities for the applications of FTIR imaging lies in its ability to study dynamic processes by making spatially resolved IR "snapshots" as a function of time. The feasibility of such an approach has recently been successfully demonstrated by Koenig and co-workers, who measured diffusion in polymers and studied polymer dissolution in mixed organic solvents.[7,12,20,21] Their work inspired our current imaging study of polymer/drug systems in contact with aqueous solution. Unfortunately, their transmission methodology would be challenging to implement for studying aqueous solutions due to the strong absorption of water in the mid-infrared. This will necessitate the use of very short path lengths which may hinder the overall dissolution process. Our approach to study polymer/drug formulations in contact with water is based on the combination of FTIR imaging in its macro mode and the ATR−IR approach. The evanescent wave that forms in ATR−IR spectroscopy probes a quite shallow layer of the sample and typically ranges from a fraction to a few micrometers. Therefore, ATR−IR spectroscopic imaging is particularly well-suited for studying aqueous solutions. It is also important to note that a dynamic system, such as in polymer dissolution

* Corresponding author: e-mail s.kazarian@imperial.ac.uk.

10.1021/ma035210l CCC: $25.00
Published on Web 12/06/2003

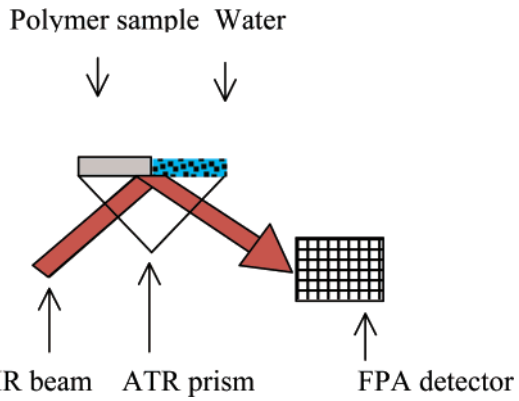

Figure 1. Schematic presentation for studying the polymer–water interface using the macro-ATR-imaging approach.

and drug release, would change during the time of the measurement needed to obtain one image. Fast acquisition in FTIR imaging allowed us to study relatively fast dissolving systems such as formulations based on poly(ethylene glycol) (PEG)—one of the most common polymers used for solid dispersions of drug.[4,22]

Experimental Section

We have used the imaging system comprising the IFS 66/S step-scan interferometer (Bruker Optics) interfaced with the macrochamber equipped with a focal plane array (FPA) MCT infrared detector (64 × 64 pixels). The spectral resolution was 16 cm^{-1}, the frame rate was 210 Hz, and the number of co-additions for each step was five.

Ibuprofen impregnated in poly(ethylene glycol) (PEG) has been used as a model drug/polymer system to represent a system for the drug with low solubility in water. Ibuprofen was supplied by Whitehall International. PEG of average molecular weights 1450 and 8000 has been purchased from Sigma. Methyl-β-cyclodextrin was kindly supplied by Wacker-Chemie GmbH. In addition, sodium benzoate was used as a model of a water-soluble drug. A heated single-reflection (incident angle of 45°) ATR (attenuated total reflectance) accessory with ZnSe crystal (Specac Ltd.) has been utilized to measure the FTIR spectra. We have recently shown[19] that such geometry of the crystal will stretch the image in one direction, and an aspect ratio correction of 1.4 is required. The film of polymer/drug formulation has been attached to the ZnSe crystal in a way to ensure good contact of the polymer sample with the ATR crystal so that water would not leak into the space between the polymer and crystal. The reproducible contact between polymer film and ATR crystal was verified by measuring the absorbance of the polymer spectral bands for several prepared films. The absorbance of the polymer bands for different films of the same polymer remained almost the same in these measurements. The polymer film was then surrounded by relatively thin spacers (a few hundred micrometers) and was covered by glass in such a way that water enters only from the side. Half of the area on the ATR crystal to be measured via the FPA detector was left uncovered by the polymer for adding water. It is important to emphasize that in this imaging arrangement we avoid the use of microscope objectives. Thus, the spatial resolution would indeed be determined by the pixel size of the FPA detector. This detector has 64 × 64 pixels, each pixel of 62 × 62 μm^2 size. Thus, infrared spectra from the sample's 4096 domains were collected and measured directly with the corresponding FPA's 4096 pixel. Figure 1 schematically shows how a large area of the drug-containing polymer sample in contact with water was measured using the FPA infrared detector. The temperature of the experiments was 40 °C.

First, we demonstrate the feasibility of the ATR–IR imaging approach to measure an interfacial area between polymer PEG and water. The image of the interfacial area between the PEG sample and water a few minutes after water was added is presented in Figure 2. The image on the right is based on the integration of the selected IR band of the polymer. The integration of the band of the polymer was chosen in the range 1170–1020 cm^{-1}. It is important to note that it is relatively straightforward to differentiate between solid and dissolved polymer due to the changes in the band shape. The image also shows representative spectra from three different areas: area of liquid water (blue), area of dissolved polymer (green), and area of the solid polymer (red). Indeed, the selected spectra in any of the "green" locations show that the band of PEG in the region of 1170–1020 cm^{-1} loses its distinct sharp features that are present in the spectrum of PEG measured in any of the "red" locations of the sample corresponding to the solid polymer. In fact, spectra of the dissolved PEG exhibit some other changes compared with the spectra of solid PEG such

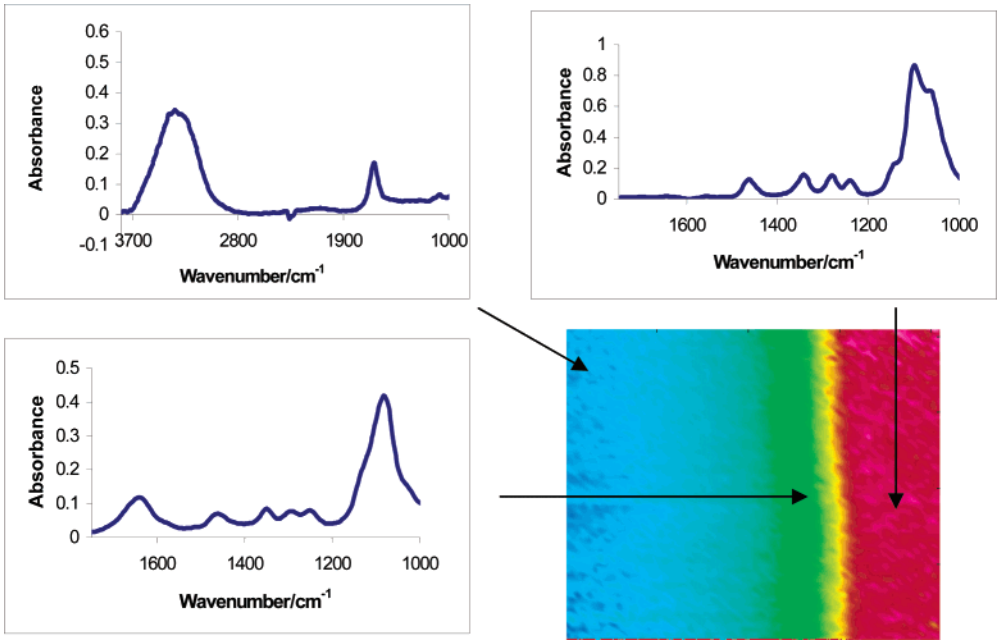

Figure 2. Representative IR spectra measured simultaneously from the different indicated locations in the sample of PEG film in contact with water (top left spectrum shows the IR spectrum of water; top right shows the region of the IR spectrum of solid polymer; bottom left shows the region of the IR spectrum of the dissolved polymer and water).

as shift and broadening of a number of spectral bands. Thus, the molecular state of the polymer (solid or dissolved) can be easily verified in any of the measured locations in the sample. Representative spectra also show the presence of the water band at ca. 1635 cm^{-1} in the sample locations where polymer is dissolved and the absence of water in the locations of the solid polymer. These spectral differences enabled us to verify that water does not leak into the space between the polymer and ATR crystal. Careful analysis of the IR spectra corresponding to the green areas in Figure 2 showed spectral bands of the dissolved PEG, thus providing evidence that the polymer film does not simply delaminate upon water diffusion into the polymer film.

The ATR−IR spectrum measured in the area far from the polymer/water interface shows the typical spectrum of liquid water. It should be noted that the molar absorptivity of the polymer bands are usually pronounced for bands corresponding to the vibrations of polar functional groups such as hydroxyl and carbonyl moieties and is not expected to be significant for the band of PEG centered at ca. 1100 cm^{-1} which results from the coupled stretching modes ν(C−O), ν(C−C) and deformation $\delta(CH_2)$ modes. The band at ca. 1060 cm^{-1} is typical of the crystalline PEG band which disappears upon dissolution or melting.[23] It should also be noted that the mode corresponding to the ν(C−OH) due to the presence of terminal OH groups in PEG also absorbs at ca. 1060 cm^{-1}, but this band is usually not pronounced for PEG samples with relatively higher molecular weight (1000 and higher). Thus, the integral absorbance of the PEG band in the range 1170−1020 cm^{-1} provides information on the concentration of PEG, and thus images based on the distribution of the absorbance of the PEG band effectively represent the image of the spatial distribution of concentration of PEG in the field of view measured via the FPA detector. This image also shows that the position of the advancing dissolving front of polymer can be measured as a function of time. This approach was used by Koenig to study mechanism of dissolution of polymers in organic solvents.[7,8,10,12,21] The plot for the dissolving interfacial front position of pure PEG in water as a function of time was neither case II nor Fickian, implying an anomalous mechanism of the dissolution. We would like to stress, however, that elucidation of the exact mechanism of the dissolution of pure PEG was not the objective of the current work. Rather, we demonstrate the principle, method, and its potential to study polymer dissolution in water via FTIR imaging but apply this method to study dissolution of polymer/drug formulations with the focus on the drug release.

Results and Discussion

Drug dissolution rates can be enhanced by the preparation of solid dispersions of drug in a water-soluble polymer matrix.[1−4,24−26] However, the actual performance of solid dispersion in drug delivery was often unpredictable due to a cited lack of basic understanding.[4] It has been shown that reduction in drug crystallite size may increase the overall drug dissolution rates. It is believed that ideally the drug needs to be dispersed in a polymer as very small particles with a dimension down to the molecular level. This is usually difficult to achieve via conventional methods of preparation of solid dispersions. Fortunately, there is a way to prepare solid formulations with a molecularly dispersed drug via supercritical fluid impregnation. We have recently shown that supercritical fluid impregnation of ibuprofen into poly(vinylpyrrolidone)[27] and PEG[28] results in formulations free of the solid drug crystallites while conventional preparation produces polymer/drug formulations where some amount of crystalline drug is still present. It has also been demonstrated that supercritical CO_2 reduces the melting temperature of PEG and assists impregnation of drug molecules from solution in CO_2. Once the process is complete, CO_2 leaves the polymer, the polymer solidifies, and the drug molecules are trapped within a polymer matrix without forming crystallites. Therefore, a film of supercritical fluid impregnated ibuprofen in PEG has been chosen to study via FTIR imaging. A sample of PEG (M_w = 8000) with impregnated ibuprofen (ca. 20 wt %) in which the absence of the drug crystalline form was evident by the position of the ν(C═O) band at 1730 cm^{-1} rather than at 1705 cm^{-1}, which would be characteristic of the crystalline ibuprofen. The shift of the ibuprofen carbonyl band to the high-wavenumber region indicates that the strong ibuprofen−ibuprofen interactions corresponding to the crystalline form are broken. Figure 3 shows images based on the distribution of the absorbance of the ν(C═O) band of the ibuprofen with integration from 1760 to 1665 cm^{-1} (bottom row) and the distribution of the absorbance of the band of PEG with integration from 1170 to 1020 cm^{-1} (top row) as a function of time. (The shape of the film was circular, and the whole film was measured in the field of view of the FPA detector.) At time t = 0 the images have been obtained just before water was added. The bottom left image shows uniform distribution of the ibuprofen in PEG. The dissolution of PEG can be observed via the images in the top row. It should be noted that in this case the geometry of the studied film makes it possible for the dissolving front of water surrounding the sample to advance from all directions as shown in Figure 3; thus, all the polymer is dissolved within 40 min despite its relatively high molecular weight. The most interesting observations concern the images (bottom row) based on the spectral band of the drug. These images show that as the polymer dissolves, the drug accumulates in the region of the initial surface layer. The images also show that, despite the fact that the polymer dissolves quite uniformly, the distribution of drug does not appear to parallel the distribution of polymer. Moreover, careful analysis of the IR spectra in the "red" areas of the bottom row in Figure 3 showed that the ν(C═O) band of ibuprofen absorbs at ca. 1705 cm^{-1} after the polymer is dissolved while the spectra in the areas where dissolved PEG is present show a very weak ν(C═O) band that appears at ca. 1720 cm^{-1}, and in the areas where polymer is not dissolved yet spectra show a stronger band at 1730 cm^{-1}. We interpret this as evidence of the drug crystallization (red areas) with precipitation of the drug crystallites on the ATR crystal. Indeed, test experiments have been performed with ibuprofen dissolved in water, and essentially no presence of the band at 1705 cm^{-1} was detected for the solution.

The integration range for ν(C═O) of ibuprofen would ensure that the effects of the shift of the ν(C═O) band as a result of crystallization, interaction with water in solution or interaction with dissolved PEG, are taken into account, and indeed the distribution of all forms of ibuprofen is presented. The size of the formed drug crystallites appears in the range 100−300 μm. This relatively large size of the drug crystallites will reduce the rate of the drug dissolution in the aqueous environment. The drug crystallization, settling, and building up to a high concentration at the surface layer have been implied[29,30] in the analysis of the mechanism of drug release from solid dispersions, but this paper reports for the first time direct experimental evidence. It should be noted that the recrystallization suggested earlier has occurred on cooling[4] while in this case the drug crystal-

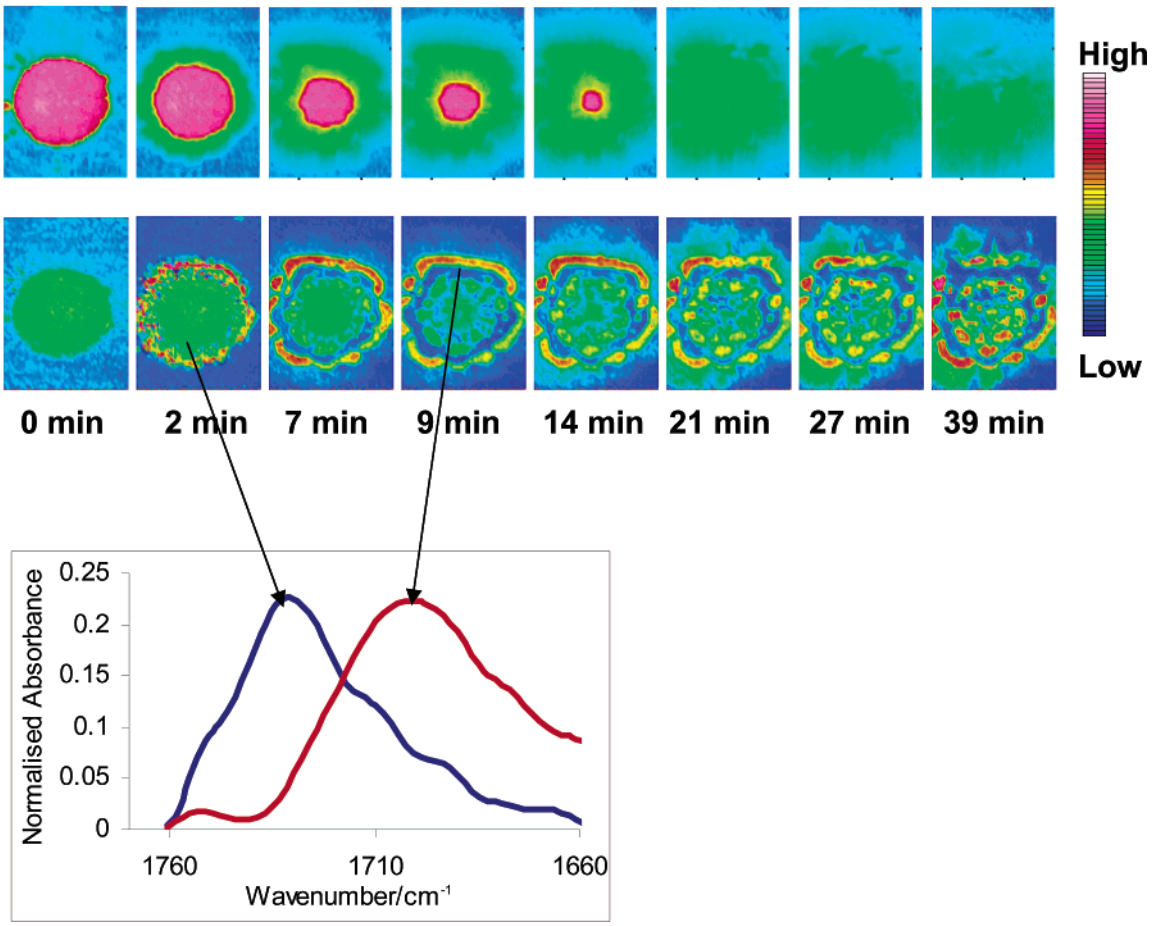

Figure 3. Macro-ATR−IR images of PEG/ibuprofen formulation show distribution of PEG and ibuprofen as a function of time during contact with water. The images (size 3.8 × 5.3 mm^2) are based on the distribution of the integral absorbance of the IR band of PEG-8000 (top row, spectral band integration from 1170 to 1020 cm^{-1}) and based on the distribution of the integral absorbance of the ν(C═O) band of ibuprofen (bottom row, integration from 1760 to 1665 cm^{-1}) acquired sequentially as a function of time. The right-hand column is the relative concentration scale. The inset shows representative IR spectra in the ν(C═O) region of ibuprofen to demonstrate spectral difference between molecularly dispersed and crystalline drug.

lized without cooling. Apparently, sparingly soluble ibuprofen quickly reaches its solubility limit as erosion/dissolution of polymer occurs due to its rather fast dissolution rate. This would lead to the saturation and consequently to the precipitation of the solid drug. The dissolution of the drug crystallites is then limited by the dissolution of the drug itself. The release of ibuprofen from dispersions in PEG has been studied via conventional methods, and it has been reported that the release rate depends on the PEG molecular weight and the weight fraction of the loaded drug. Recent studies implied that the release rate of the amorphous drug can be much slower than the release of drug dispersed as crystallites. This could be explained as a recrystallization of the amorphous drug forming a continuous drug-enriched layer that inhibits dissolution of the remaining part of the sample. It is important to note that convection was essentially absent in our ATR−IR imaging approach. This could result in slowing the rate of the polymer dissolution due to formation of the gel-like layer next to the area of the solid polymer.[31] Koenig and coworkers also mentioned[12] that polymer chains remaining at the polymer−solvent interface decrease the overall dissolution rate and that convection would affect the rate of dissolution when the dissolved layer is greater than a few hundred microns (as in our case). Our experimental approach allows incorporation of a flow cell on top of the ATR crystal, thus inducing convective flows, and this will be explored in future studies. Despite the success of our ATR−IR imaging approach, we also attempted to study the release of ibuprofen from PEG using the IR transmission cell with the possibility of flow. This was needed in order to prove that the observation of the crystallized drug layer is not the result of an artifact of the ATR−IR method, such as affinity of the drug to the ATR crystal with consecutive precipitation of the drug on the surface of the crystal. Although transmission measurements of aqueous systems are challenging, given a relatively short path length (ca. 6 μm), one could, in principle, use weak bands of the polymer and drug that are not obscured either by bands of water or by the stronger bands of the polymer. The advantage of the transmission approach is that one can also obtain a visible image of the sample and compare or overlay this with the acquired FTIR images. The resulting images are shown in Figure 4. The images obtained before addition of water show a homogeneous distribution of both ibuprofen and PEG.

However, the images obtained after 1.5 h show the segregation of drug with the formation of the drug-enriched layer surrounding nondissolved area of the sample. Similar images were first obtained after 40 min and hardly changed later, indicating that a stagnant layer was formed due to the drug crystallization. It is clear that such a layer would indeed impede the dissolution of the remaining part of the sample. To prove

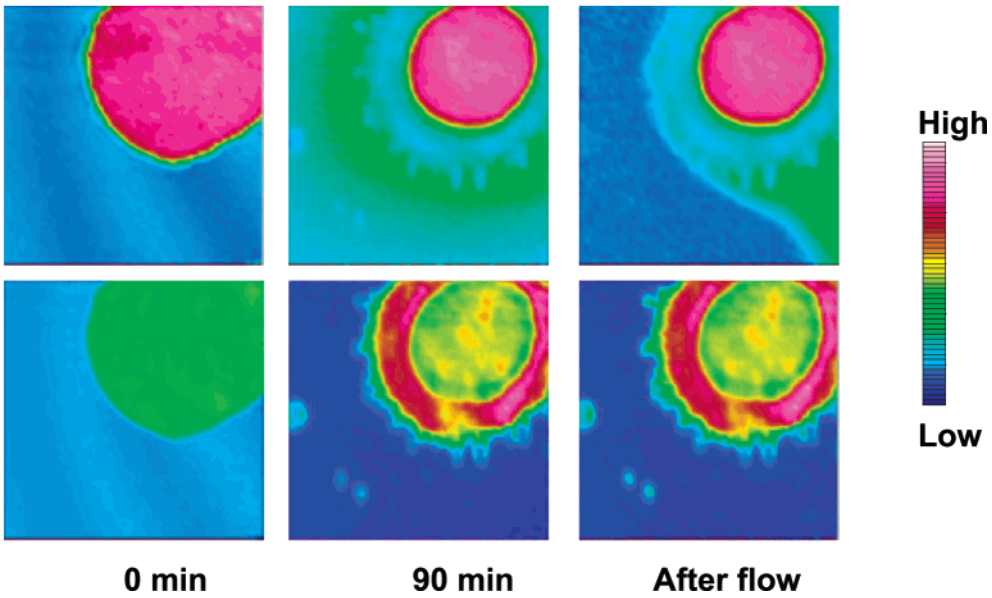

Figure 4. Transmission FTIR images (3.8 × 3.8 mm^2) of ibuprofen/PEG show distribution of PEG (top row) and ibuprofen (bottom row). The images on the left are obtained before addition of water. Images in the center were measured after 90 min contact with water. Images on the right were measured after flow of water was applied in the transmission cell which has affected distribution of PEG outside layer of crystalline drug (shown by a red ring) but had no effect on drug and polymer encircled by the drug layer.

that the gel layer of the polymer (indicated by the green outer circle in the top image) surrounding the drug-enriched layer (red circle layer in the bottom images) does not play a major role in preventing drug release, the flow of water was applied through the transmission IR cell. The FTIR image obtained immediately after such flow shows that although flow has removed most of the gel layer of PEG surrounding nondissolved parts of the sample, it had no effect on the drug-enriched layer and the remaining solid sample. This image remained essentially unchanged after some time, supporting our argument that it is the drug-enriched layer that prevents further dissolution of the sample. These measurements also highlight the inherent problem of using spectroscopic imaging in transmission to study aqueous solutions. As Figure 4 shows, the small path length of the transmission cell results in the crystallized ibuprofen, almost completely blocking access of water to the rest of polymer/drug formulation. Our ATR−IR imaging approach did not have this limitation, and the formation and growth of the drug crystallites were not a result of a being confined in space and did not prevent access of water to the center of the sample. It might seem that the ability of the ATR−IR approach to detect the substances only in close vicinity to the surface of the ATR crystal is a limitation of the technique. However, this may actually be an advantage as this approach analyzes the physiologically relevant situation to the distribution of the drug on the surface of the gastrointestinal track rather than the distribution of the drug in the whole volume of the surrounding fluids.

Next we consider FTIR imaging of the system with water-soluble substances incorporated into PEG to demonstrate that the observed drug crystallization is limited to substances with low solubility in water. We chose sodium benzoate (SB) as a model material because of its high solubility in water, suitable IR bands to monitor its release, and due to the fact that it is frequently used as antimicrobial preservative and tablet lubricant. The formulation of PEG with ca. 22% of SB was prepared by melting. The spatial distribution of SB as a function of time was followed using the band at 1550 cm^{-1}, corresponding to the antisymmetric vibration of the COO moiety in SB. Figure 5 shows images based on the distribution of the spectral absorbance of SB and PEG as a function of time.

There is a remarkable similarity between these images showing that both drug and polymer dissolve almost simultaneously. This could imply that drug release proceeds via polymer dissolution rather than diffusion of drug through the polymer. In any case there was no evidence of formation of the drug-enriched layer as was observed for the release of the ibuprofen. Therefore, these results may imply that it is the solubility of a drug that is essential if the formation of the drug-enriched layer is to be prevented. The release of ibuprofen from dispersions in PEG has been studied via conventional methods,[32] and it has been reported that the release rate depends on the PEG molecular weight and the weight fraction of the loaded drug. However, the reduction of molecular weight of PEG from 8000 to 4000 did not show a significant effect on formation of crystalline ibuprofen. Reducing ibuprofen/PEG ratio or pH of aqueous solution, adding NaCl into solution, and mixing surfactant or talc with the formulation also did not have a noticeable effect on crystallization of ibuprofen. It is important to note that although formulation of PEG/ibuprofen in contact with water represents a model system for studying drug release, the change of pH (via addition of HCl) and adding NaCl allowed us to mimic physiologically relevant conditions of solvent using our in vitro approach.

Cyclodextrin and its derivatives are known to be able to enhance dissolution rates of certain drugs due to their ability to entrap molecules of certain drugs within the internal cavity of cyclodextrin moiety.[33] Foster and coworkers[34] reported the enhancement of dissolution rate of ibuprofen from its inclusion complex formation with methyl-β-cyclodextrin (MBCD). The enhanced dissolution rate in that work was assigned to the amorphous nature of the product and improved wettability. In this work the ATR−IR imaging was applied to monitor the

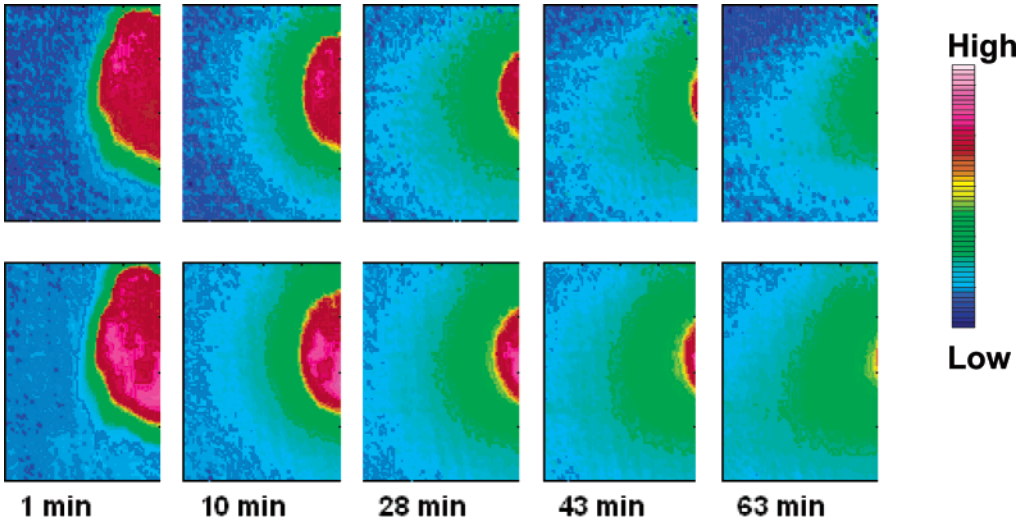

Figure 5. Macro-ATR−IR images of PEG/sodium benzoate showing distribution of sodium benzoate (top row) and PEG (bottom row) as a function of time. The images 3.8 × 5.3 mm^2 for sodium benzoate are based on the integral absorbance of the band from 1574 to 1510 cm^{-1}.

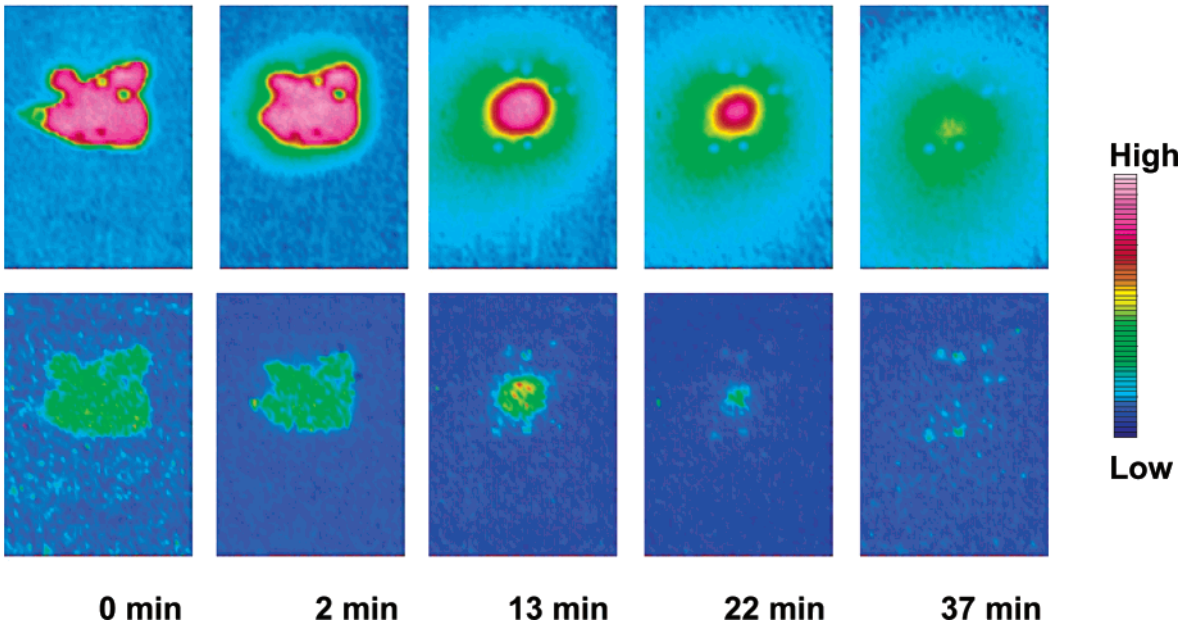

Figure 6. Macro-ATR−IR images of MBCD/ibuprofen showing distribution of MBCD (top row) and ibuprofen (bottom row) as a function of time during contact with water. The images 3.8 × 5.3 mm^2 demonstrate almost total dissolution of ibuprofen after 40 min contact with water.

process of dissolution of an ibuprofen/MBCD complex to investigate whether this complex would prevent the crystallization of ibuprofen. Figure 6 shows images based on the distribution of the absorbance of the MBCD band (top row) and the distribution of the absorbance of the carbonyl band of ibuprofen (bottom row) as a function of time. The images on the left (at $t = 0$) have been obtained just before water was added. The observed dissolution pattern of MBCD is rather similar to the dissolution pattern of PEG while the corresponding images based on the distribution of ibuprofen in the bottom row did not show any evidence of crystallization (although the amount of drug was comparable to that used in the experiment with PEG). In fact, the images show the apparent "disappearance" of the ibuprofen as MBCD dissolves. However, it should be noted that the volume of the water surrounding the sample is much greater than the volume of the sample. The implication of this is that dissolved MBCD and ibuprofen disappear from the imaging area due to partitioning into the aqueous environment as the aqueous area does not reach saturation with the amount of the polymer sample used in this experiment.

Most importantly, these measurements prove that using an inclusion complex (molecular ratio of ibuprofen/MBCD not higher than 1:1, which corresponds to 12 wt % of drug) does prevent crystallization of ibuprofen since the molecules of MBCD are able to aid sample dispersal prior to decomposition of MBCD and release of ibuprofen. Additional experiments have shown that an increase in the ibuprofen/MBCD ratio results in aggregation which causes the crystallization of the excess drug. These results reveal the origin of enhanced dissolution rates of ibuprofen and open new opportunities for studying controlled drug release with FTIR imaging. For example, our data with ibuprofen as a model drug provide a plausible explanation of the previously observed enhancement in dissolution of nor-

floxacin using an inclusion complex with cyclodextrins compared to solid dispersion in PEG.[35]

Conclusions and Implications

In summary, an ATR−IR imaging approach has allowed us to simultaneously study the spatial distribution of both polymer and drug in contact with water as a function of time. The important observation in our study is that crystallization of the initially molecularly dispersed drug occurs upon contact with the dissolution medium, and this slows overall drug dissolution. Such crystallization inhibits drug release and impacts its bioavailability. The intriguing conclusion is that the formation of drug crystallites and the drug-enriched layer are enhanced due to the drug being molecularly dispersed. Such a proposal was put forward by Serajuddin,[24] and our data provide the first experimental evidence for this. This may also help to understand complex behavior of solid dispersions which were prepared so far.[4] This also points to the possible value of added surface-active carriers that could emulsify and disperse drugs, thus preventing the formation of drug crystallites from formulations using water-soluble polymers. Finally, our imaging approach has allowed us to visualize dissolution of inclusion complexes of ibuprofen with cyclodextrins that allow prevention of drug crystallization. The approach described in this paper is particularly applicable to the solid dispersions of drugs in water-soluble polymers used for oral drug delivery. The potential also exists to apply the presented approach to the formulations where degradation occurs via an enzymatic mechanism. The general principles of our experimental methodology as described here will also be applicable to study transdermal drug delivery and release. Furthermore, this approach will have broader technological implications, for example, in studies of water uptake into polymers, adhesives, and personal care products and in the release of active agents such as flavors and fragrances. In addition, with recently demonstrated suitability of the diamond ATR−IR accessory for imaging application,[18] compaction of a mixture of different components to a tablet directly on the diamond and dissolution the can be studied in situ via the ATR−IR imaging approach with enhanced spatial resolution. This is the topic of our current investigations and will be reported elsewhere.

Overall, this paper described a novel macro-ATR−IR spectroscopic imaging approach that opens new opportunities for studying polymer dissolution in aqueous solution and drug release and will provide guidance to the design of pharmaceutical polymer-based formulations with tailored release properties.

Acknowledgment. We thank EPSRC for funding (Grant GR/S03942/01), Bruker Optics Ltd. and Specac Ltd. for support, Pfizer for CASE studentship to K.L.A.C., and Dr. P. Turner, Prof. J. Hadgraft (University of Greenwich), and Prof. P. F. Luckham (Imperial College London) for their help and advice.

References and Notes

(1) Siepmann, J.; Gopferich, A. *Adv. Drug Del. Rev.* **2001**, *48*, 229−247.
(2) Siepmann, J.; Peppas, N. A. *Adv. Drug Del. Rev.* **2001**, *48*, 139−157.
(3) Narasimhan, B. *Adv. Drug Del. Rev.* **2001**, *48*, 195−210.
(4) Craig, D. Q. M. *Int. J. Pharm.* **2002**, *231*, 131−144.
(5) Koenig, J. L. *Microscopic Imaging of Polymers*; American Chemical Society: Washington, DC, 1998.
(6) Koenig, J. L.; Wang, S. Q.; Bhargava, R. *Anal. Chem.* **2001**, *73*, 360A−369A.
(7) Miller-Chou, B. A.; Koenig, J. L. *Macromolecules* **2002**, *35*, 440−444.
(8) Miller-Chou, B. A.; Koenig, J. L. *Macromolecules* **2003**, *36*, 4851−4861.
(9) Salzer, R.; Steiner, G.; Mantsch, H. H.; Mansfield, J.; Lewis, E. N. *Fresenius J. Anal. Chem.* **2000**, *366*, 712−726.
(10) Snively, C. M.; Koenig, J. L. *J. Polym. Sci., Part B: Polym. Phys.* **1999**, *37*, 2261−2268.
(11) Kazarian, S. G.; Higgins, J. S. *Chem. Ind.* **2002**, *10*, 21−23.
(12) Ribar, T.; Bhargava, R.; Koenig, J. L. *Macromolecules* **2000**, *33*, 8842−8849.
(13) Narasimhan, B.; Snaar, J. E. M.; Bowtell, R. W.; Morgan, S.; Melia, C. D.; Peppas, N. A. *Macromolecules* **1999**, *32*, 704−710.
(14) Malveau, C.; Beaume, F.; Germain, Y.; Canet, D. *J. Polym. Sci., Part B: Polym. Phys.* **2001**, *39*, 2781−2792.
(15) Fyfe, C. A.; Grondey, H.; Blazek-Welsh, A. I.; Chopra, S. K.; Fahie, B. J. *J. Controlled Release* **2000**, *68*, 73−83.
(16) Baille, W. E.; Malveau, C.; Zhu, X. X.; Marchessault, R. H. *Biomacromolecules* **2002**, *3*, 214−218.
(17) Wetzel, D. L.; Reffner, J. A. *Chem. Ind.* **2000**, *9*, 308−313.
(18) Chan, K. L. A.; Hammond, S. V.; Kazarian, S. G. *Anal. Chem.* **2003**, *75*, 2140−2147.
(19) Chan, K. L. A.; Kazarian, S. G. *Appl. Spectrosc.* **2003**, *57*, 381−389.
(20) Rafferty, D. W.; Koenig, J. L. *J. Controlled Release* **2002**, *83*, 29−39.
(21) Koenig, J. *Adv. Mater.* **2002**, *14*, 457−460.
(22) Leuner, C.; Dressman, J. *Eur. J. Pharmacol. Biopharm.* **2000**, *50*, 47−60.
(23) Matsuura, H.; Miyazawa, T. *J. Polym. Sci., Part A-2* **1969**, *7*, 1735−1744.
(24) Serajuddin, A. T. M. *J. Pharm. Sci.* **1999**, *88*, 1058−1066.
(25) Corrigan, O. I. *Drug Dev. Ind. Pharm.* **1985**, *11*, 697−724.
(26) Margarit, M. V.; Rodriguez, I. C.; Cerezo, A. *Int. J. Pharm.* **1994**, *108*, 101−107.
(27) Kazarian, S. G.; Martirosyan, G. G. *Int. J. Pharm.* **2002**, *232*, 81−90.
(28) Kazarian, S. G. *Macromol. Symp.* **2002**, *184*, 215−228.
(29) Dubois, J. L.; Ford, J. L. *J. Pharm. Pharmacol.* **1985**, *37*, 494−495.
(30) Sertsou, G.; Butler, J.; Hempenstall, J.; Rades, T. *J. Pharm. Pharnacol.* **2002**, *54*, 1041−1047.
(31) Narasimhan, B.; Peppas, N. A. *J. Pharm. Sci.* **1997**, *86*, 297−304.
(32) Shakhtshneider, T. P.; Vasiltchenko, M. A.; Politov, A. A.; Boldyrev, V. V. *Int. J. Pharm.* **1996**, *130*, 25−32.
(33) Rao, V. M.; Stella, V. J. *J. Pharm. Sci.* **2003**, *92*, 927−932.
(34) Charoenchaitrakool, M.; Dehghani, F.; Foster, N. R. *Int. J. Pharm.* **2002**, *239*, 103−112.
(35) Guyot, M.; Fawaz, F.; Bildet, J.; Bonini, F.; Lagueny, A. M. *Int. J. Pharm.* **1995**, *123*, 53−63.

MA035210L